X-910-75-129
PREPRINT

A SIMPLE METHOD TO INCORPORATE WATER VAPOR ABSORPTION IN THE 15 μm REMOTE TEMPERATURE SOUNDING

G. DALU
C. PRABHAKARA
B. J. CONRATH

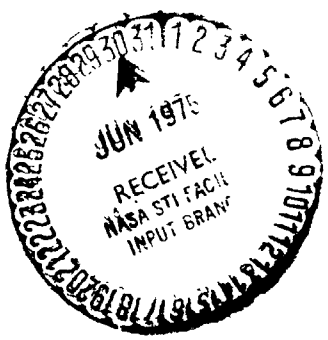

MAY 1975

GSFC
GODDARD SPACE FLIGHT CENTER
GREENBELT, MARYLAND

A SIMPLE METHOD TO INCORPORATE WATER VAPOR ABSORPTION IN THE 15 μm REMOTE TEMPERATURE SOUNDING

G. Dalu*

C. Prabhakara

B. J. Conrath

ABSTRACT

The water vapor absorption in the 15 μm CO_2 band, which can affect the remotely sensed temperatures near the surface, can be estimated with the help of an empirical method. This method is based on the differential absorption properties of the water vapor in the 11-13 μm window region and does not require a detailed knowledge of the water vapor profile. With this approach Nimbus 4 IRIS radiance measurements are inverted to obtain temperature profiles. These calculated profiles agree with radiosonde data within about 2°C.

*Computer Sciences Corporation. Present address: C.N.R. - Istituto di Fisica dell'Atmosfera - Rome, Italy.

CONTENTS

ILLUSTRATIONS

TABLES

TABLES (Continued)

A SIMPLE METHOD TO INCORPORATE WATER VAPOR ABSORPTION IN THE 15 μm REMOTE TEMPERATURE SOUNDING

INTRODUCTION

Temperature sounding, from remotely sensed infrared radiances in the 15 μm CO_2 band, has been a significant advancement in the field of meteorology. Several investigators (Wark and Hilleary, 1969; Hanel and Conrath, 1969; Conrath, et al., 1970; Smith, et al., 1970; Wark, 1970) have developed techniques to invert the 15 μm radiances to derive temperature profiles. In the 15 μm band there is some absorption due to water vapor. In the earlier studies mentioned above, a water vapor profile was used to account for such absorption.

Retrieval of the water vapor profile from remote measurements in one of the water vapor absorption bands, in turn, requires the temperature profile. Thus the solution to the problem of temperature sounding from the 15 μm data becomes one of an iterative nature. It will be helpful to avoid this iteration.

Water vapor decreases rapidly above the surface with a scale height of about 2 km. Contrary to this fine scale, the vertical resolution of the retrieved temperature profile (Conrath, 1972) from the 15 μm band is a few kilometers near the surface. In view of these facts, accurate representation of the water vapor profile near the surface is not necessary for the temperature sounding. Furthermore the 11-13 μm window measurements, which can be used to estimate the surface temperature (Prabhakara, et al., 1974) allow us to estimate the

absorption due to water vapor. With this information, a simple method is developed in the present study which utilizes the window measurements in the 11-13 μm region to assess the water vapor absorption in the 14 μm wing of the CO_2 band without an interative procedure. The problem of temperature sounding is thus uncoupled from the water vapor sounding.

Nimbus 4 IRIS spectra (Hanel, et al., 1972) have been used to test the method developed, but comparable results are expected from multi-channel radiometer measurements.

METHOD

In Figure 1, a spectrum measured by IRIS over Guam on April 27, 1970 in the spectral region 600 to 1000 cm^{-1} is shown.

Utilizing radiosonde measurements over Guam on that day, the absorption due to water vapor is calculated with a line by line integration program of Kunde and Maguire (1974) and is shown in the same figure. From this figure one can readily see the magnitude of water vapor absorption in the 15 μm band which can be significant particularly over the tropics. Near the middle of the band, the CO_2 weighting functions peak in the stratosphere or upper troposphere (Conrath, 1972). This can be easily inferred from the set of blackbody emission curves included in the figure. Hence the absorption due to the water vapor present in the lower troposphere is unimportant. However, the weighting functions for CO_2 in the 14 μm region of the band, from about 725 to 770 cm^{-1}, peak in the lower

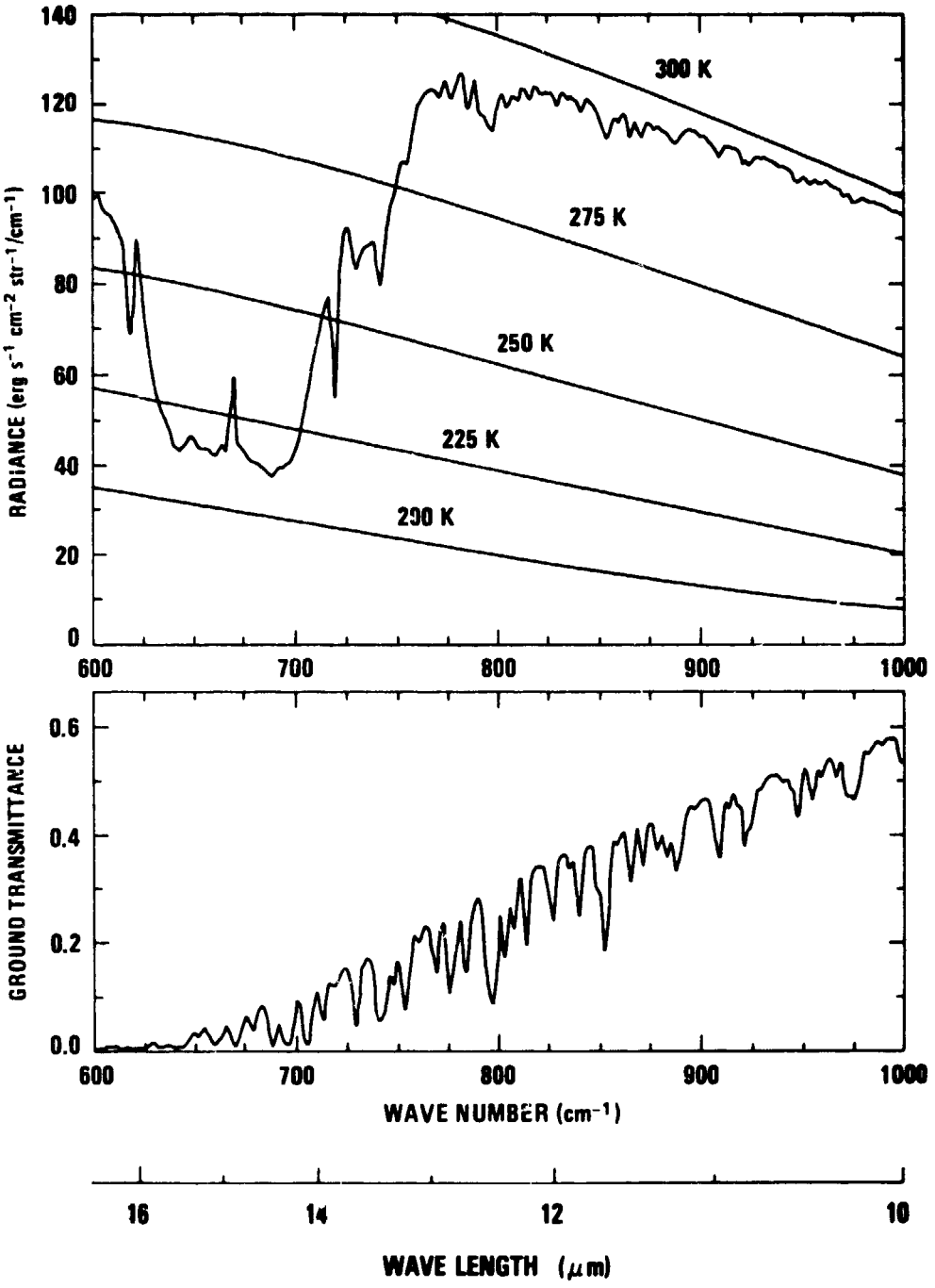

Figure 1. Cloud-free Nimbus 4 IRIS spectrum taken over the ocean on April 27, 1970 at 15.1°N and 144.7°W (GUAM), and the blackbody emission curves. The water vapor transmittance calculated with the radiosonde data is also shown.

troposphere or near the surface and the water vapor absorption should be taken into account.

From the transmission curve of the water vapor displayed in Figure 1, one can also see that there is a simple trend to the curve from 11 to 14 μm. Since CO_2 has negligible absorption in the 11-13 μm window, radiance measurements in this region can give some information on the water vapor absorption in the atmosphere. Also the surface temperature can be estimated with these window measurements (Prabhakara, et al., 1974, subsequently referred to as PDK). With the help of this information, we can assess the water vapor absorption in the 14 μm region which is spectrally adjacent to the window.

By considering the water vapor continuum absorption to be dependent on vapor pressure and total pressure, and also the absorption due to spectral lines, PDK have shown empirically that the transmission τ in the window from 775 to 960 cm^{-1} can be linearly related to the amount of precipitable water $w(g\,cm^{-2})$ in the atmosphere as

$$\tau_\nu \cong 1 - k_\nu w \qquad (1)$$

where k_ν $(cm^2\,g^{-1})$ is a relative absorption coefficient. Also from similar calculation of the water vapor transmission in the 725-775 cm^{-1} region, it is found that the approximation expressed by Equation (1) is valid. The values of $k(\nu)$ used in this study are listed in Table 1.

Table 1

Relative Absorption Coefficient (g^{-1} cm^2) as a Function of Wave Number in the Water Vapor Window Region

$\Delta\nu(cm^{-1})$	725-730	730-735	735-740	740-745	745-750	750-755	755-760	775-831	831-887	887-960
$k(g^{-1}\ cm^2)$	0.23	0.24	0.20	0.26	0.25	0.24	0.19	0.191	0.131	0.104

In a cloud-free, non-scattering atmosphere under local thermodynamic equilibrium, the radiative equation for the upwelling intensity $I(\nu)$ may be written as

$$I(\nu) = B(\nu, T_o)\, \tau(\nu, p_o) + \int_{\tau(\nu, p_o)}^{1} B[\nu, T(p)]\, d\tau(\nu, p) \qquad (2)$$

where p_o and p are surface pressure and pressure at any height, respectively (mb),

ν is the wave number (cm^{-1}),

T is the temperature (K),

T_o is the surface temperature (K),

B is the Planck intensity (erg cm^{-1} $ster^{-1}$ s^{-1}),

τ is the transmission from any pressure level p to the top of the atmosphere.

The surface emissivity is assumed to be unity.

For the window region, the integral in Equation (2) can be simplified and then the equation can be rearranged suitably to give

$$\frac{I(\nu)}{B(\nu, T_o)} = \tau(\nu, p_o) \left(1 - \frac{\bar{B}(\nu)}{B(\nu, T_o)}\right) + \frac{\bar{B}(\nu)}{B(\nu, T_o)} \qquad (3)$$

where

$$\bar{B}(\nu) = \frac{\displaystyle\int_{\tau(\nu, p_o)}^{1} B[\nu, T(p)]\, d\tau(\nu, p)}{\displaystyle\int_{\tau(\nu, p_o)}^{1} d\tau(\nu, p)} \qquad (4)$$

is the effective emission of the water vapor layer near the surface.

In the window, the ratio of $I(\nu)/B(\nu, T_0)$ is a function of the total transmission of water vapor in the atmosphere and the temperature distribution. The dependence on the temperature distribution is contained in $\bar{B}(\nu)$. As the water vapor content in the lower atmosphere varies with height much more rapidly than the temperature, the water vapor distribution critically determines $\bar{B}(\nu)$.

From Equations (1) and (3) we have

$$\frac{I(\nu)}{B(\nu, T_0)} = 1 - k(\nu)\, F(w, \nu, T_0) \tag{5}$$

where

$$F(w, \nu, T_0) = w\left(1 - \frac{\bar{B}(\nu)}{B(\nu, T_0)}\right) \tag{6}$$

The water vapor content w and the effective emission $\bar{B}(\nu)$ are not related in a simple fashion. However if we use the integration program of Kunde and Maguire (1974) for some typical average atmospheric models, we find that the water vapor content w and the function $F(w, \nu, T_0)$ are correlated in a simple way. In the graph of Figure 2 the values of w and F are plotted for the 831-887 cm^{-1} window region for an average tropical atmosphere (T on the graph), for an average mid-latitude atmosphere (MS) in the summer, and an average midlatitude atmosphere in the winter (MW). The temperature and water vapor profiles used for these model calculations are given in McClatchey, et al., (1972).

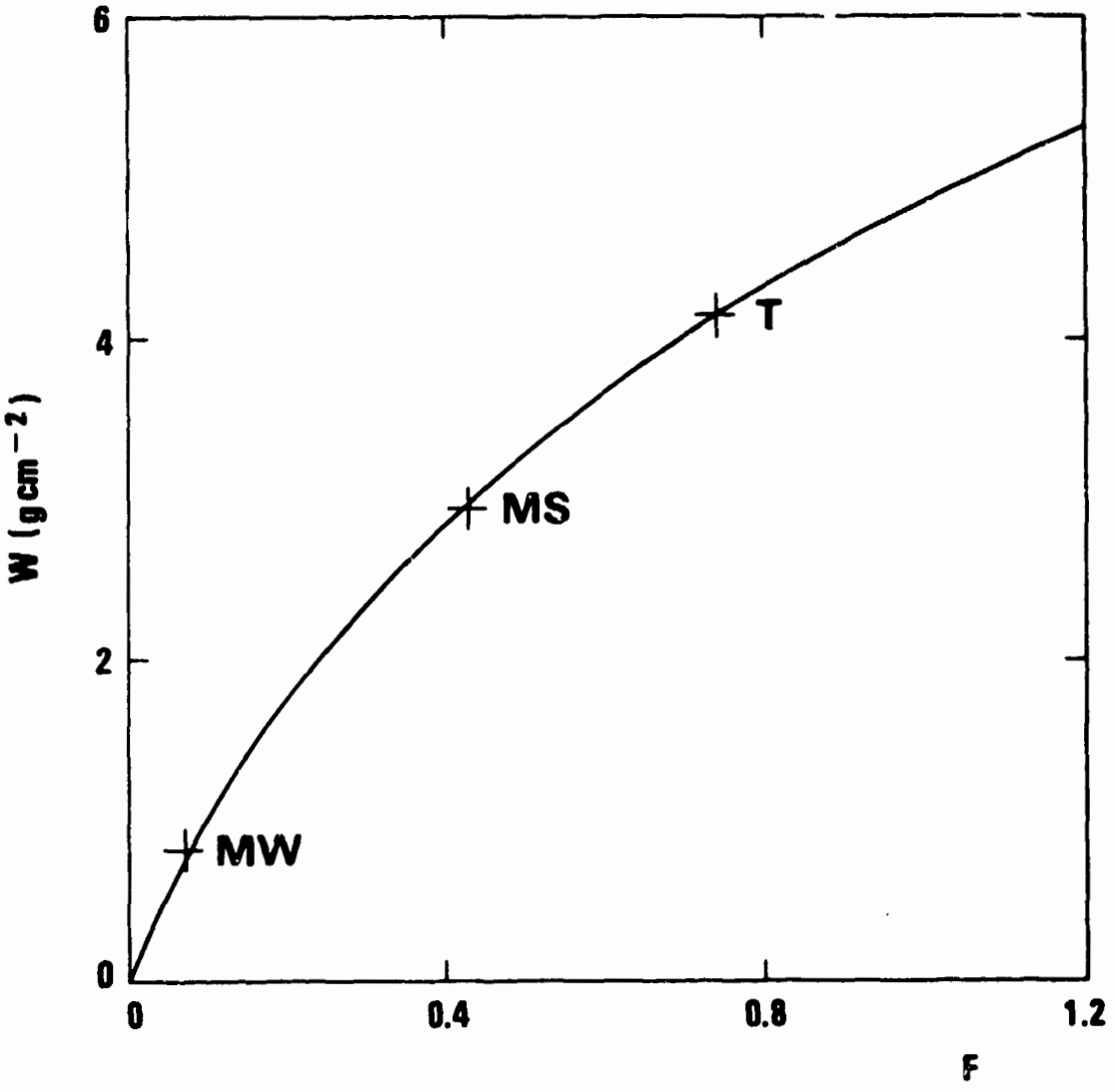

Figure 2. Relationship between the function F and the precipitable water content in the atmosphere. T is an example of tropical atmosphere, and MS and MW are midlatitude cases for summer and winter, respectively.

The surface temperature T_0 can be determined from a method developed by PDK with the help of two remote radiance measurements in the 11-13 μm window. From the measured brightness temperature in the 831-887 cm^{-1} region, the ratio $I(\nu)/B(\nu, T_0)$ can be calculated and with the help of Equation (5), the value of the function $F(w, \nu, T_0)$ is determined. The graph of Figure 2 then provides an evaluation of the parameter w, which can be used as an equivalent water vapor content.

Given the equivalent total water content w_e, it is assumed that the water vapor w(p) contained from any pressure level p to the top of the atmosphere can be related to w_e with the help of a scaling function R(p) such that

$$w(p) = R(p)\, w_e \tag{7}$$

The values used for R(p) deduced from some mean water vapor distribution are listed in Table 2.

Table 2

Scaling Function R(p) for the Water Vapor Distribution

p(mbar)	100	200	300	400	500	600	700	800	900	1000
R(p)	0.00	0.01	0.02	0.05	0.09	0.15	0.26	0.44	0.66	1.0

For the 15 μm CO_2 band, Equation (2) can be written as

$$\begin{aligned} I(\nu) = {} & B(\nu, T_0)\, \tau_{H_2O}(\nu, p_0)\, \tau_{CO_2}(\nu, p_0) \\ & + \int_{\tau_{H_2O}(\nu, p_0)}^{1} B[\nu, T(p)]\, \tau_{CO_2}(\nu, p)\, d\tau_{H_2O}(\nu, p) \\ & + \int_{\tau_{CO_2}(\nu, p_0)}^{1} B[\nu, T(p)]\, \tau_{H_2O}(\nu, p)\, d\tau_{CO_2}(\nu, p) \end{aligned} \tag{8}$$

In this equation the intensity $I(\nu)$ is measured; the value of $B(\nu, T_0)$ is estimated by using at least two channels in the 11-13 μm window region; the water vapor transmissivity $\tau_{H_2O}(\nu, p)$ is estimated with the help of Equations (1) and (7); $\tau_{CO_2}(\nu, p)$ is known, so the only unknown is T(p). Any known technique to invert Equation (8) can be used to calculate the temperature profile. In the present study we have used the technique developed by Conrath (1972).

In Equation (5), $\bar{B}$ is shown to be dependent on the temperature structure. However the equivalent water content estimated from Figure 2 can account for cases n which temperature gradients do not differ substantially from an average lapse rate of -6.5°C/km. Only in the extreme cases where there is a superadiabatic gradient or a strong inversion near the surface will this procedure be in error. Such a limitation is also inherent in the more elaborate iterative inversion techniques, because of the crude vertical resolution of the retrieved temperature profiles (Conrath, 1972).

RESULTS

The Nimbus 4 IRIS spectra were used to test the method developed. A few spectra have been selected for which the corresponding temperature profiles from radiosondes were available. The radiosonde launches were conducted within one hour and a few degrees in latitude and longitude from the spot sensed by the satellite.

As an example, the temperature profiles obtained near GUAM, latitude 15°N and longitude 145°E, on April 27, 1970, are presented in Figure 3. The solid line corresponds to the radiosonde temperature profile, while the dashed line is the corrected temperature profile obtained from the inversion of the 15 μm CO_2 band. If no correction for the water vapor absorption is introduced, i.e., this absorption is assumed to be negligible at any level, the inversion of the CO_2 band would give the deformed temperature profile shown with the dots in the same figure.

In Table 3 a few temperature profiles are listed. For each case there are three profiles: the first one was obtained with a radiosonde; the second one was calculated from the 15 μm CO_2 band, but corrected using the water vapor profile obtained from the radiosonde itself; the third one was calculated with the present method, i.e., without any data on the water vapor content of the atmosphere.

The error of the temperatures calculated from the inversion of the radiances measured from the IPIS, is about 2°K in the layers near the surface.

The correction for the water vapor absorption is actually most important between 700 mbar and the surface (Figure 3). The comparison of the profiles presented in Table 3 show differences of 1°K or less between this method and the inversion of the 15 μm band with the correction for the water vapor absorption obtained by using the water vapor profile measured with a radiosonde.

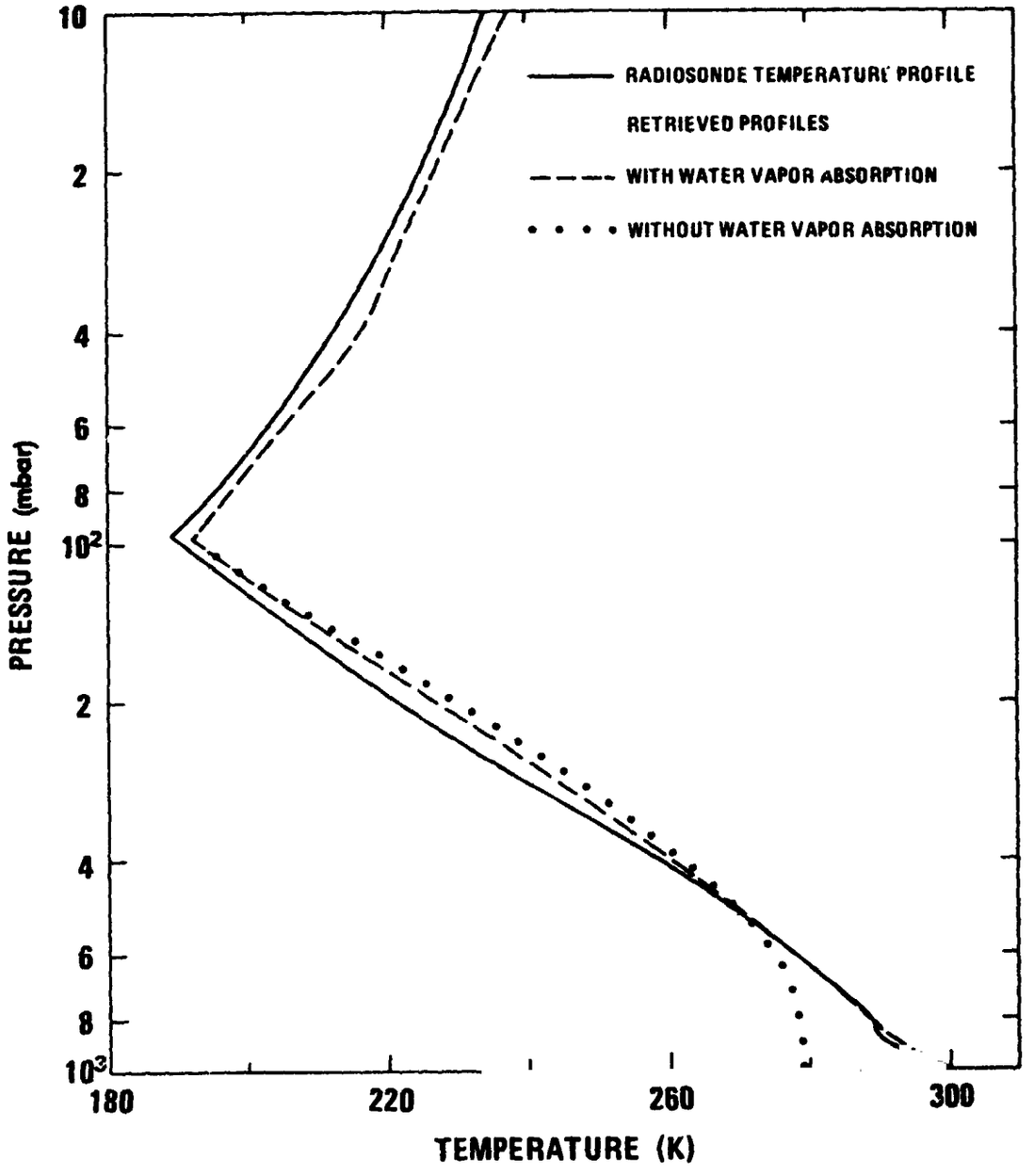

Figure 3. Comparison among the radiosonde temperature profile, the retrieved profile without water vapor correction, and the corrected temperature profile. The IRIS data used are the same presented in Figure 1 (GUAM).

Table 3

Comparison of the Present Temperature Sensing Method with the Radiosonde Measurements

Atmospheric pressure (mbar)	GUAM (2:02 G.M.T., April 27, 1970) Spectrum #139, Long 144.7 E, Lat 15.1 N Total water vapor content: 3.2 g cm^{-2}			GIBRALTAR (11:35 G.M.T., April 24, 1970) Spectrum #66, Long 3.1 W, Lat 36.1 N Total water vapor content: 1.6 g cm^{-2}		
	Radiosonde Temperature Profile (K)	Inversion with water vapor from Radiosonde (K)	Inversion with water vapor abs. correction (K)	Radiosonde Temperature Profile (K)	Inversion with water vapor from Radiosonde (K)	Inversion with water vapor abs. correction (K)
108	193.3	195.4	195.5	207.7	212.2	212.2
145	207.1	210.3	210.4	210.7	213.0	213.0
177	216.3	220.5	220.6	211.0	215.1	215.2
215	225.5	230.9	230.8	214.6	218.1	218.2
262	235.1	240.9	240.7	224.4	226.6	226.8
320	246.3	250.4	250.1	234.4	237.7	237.6
390	257.5	259.4	259.1	244.7	248.8	248.7
476	268.1	268.4	267.8	256.9	259.5	259.2
525	272.1	272.8	272.2	262.5	264.8	264.3
580	276.2	277.2	276.6	267.5	269.9	269.3

Table 3 (Continued)

Atmospheric pressure (mbar)	GUAM (2:02 G.M.T., April 27, 1970) Spectrum #139, Long 144.7 E, Lat 15.1 N Total water vapor content: 3.2 g cm^{-2}			GIBRALTAR (11:35 G.M.T., April 24, 1970) Spectrum #66, Long 3.1 W, Lat 36.1 N Total water vapor content: 1.6 g cm^{-2}		
	Radiosonde Temperature Profile (K)	Inversion with water vapor from Radiosonde (K)	Inversion with water vapor abs. correction (K)	Radiosonde Temperature Profile (K)	Inversion with water vapor from Radiosonde (K)	Inversion with water vapor abs. correction (K)
640	280.2	281.4	280.9	272.5	274.7	274.0
707	284.4	285.6	284.9	277.4	279.3	278.6
781	288.6	288.6	288.0	281.5	283.3	283.2
862	289.9	291.0	291.5	285.9	286.9	286.6
952	296.5	293.4	295.4	292.0	290.2	290.2
1013	301.1	297.0	300.0	293.0	290.0	292.8

Table 3 (Continued)

Atmospheric pressure (mbar)	BRINDISI (10:05 G. M. T., April 26, 1970) Spectrum #63, Long 17.8 E, Lat 41.7 N Total water vapor content: 0.9 g cm^{-2}			WALLOPS IS. (15:58 G. M. T., June 25, 1970) Spectrum #37, Long 69.9 W, Lat 38.9 N Total water vapor content: 2.2 g cm^{-2}		
	Radiosonde Temperature Profile (K)	Inversion with water vapor from Radiosonde (K)	Inversion with water vapor abs. correction (K)	Radiosonde Temperature Profile (K)	Inversion with water vapor from Radiosonde (K)	Inversion with water vapor abs. correction (K)
108	214.3	214.2	214.2	210.8	209.8	209.8
145	219.0	213.5	213.4	210.1	210.9	211.0
177	216.3	214.3	214.3	209.2	215.1	215.3
215	214.5	215.9	215.9	218.6	221.9	222.2
262	219.4	223.3	223.3	228.7	231.9	232.4
320	230.5	233.7	233.9	239.4	241.6	242.2
390	234.6	244.4	244.7	249.7	252.8	253.3
476	250.9	255.2	255.9	261.1	263.6	263.8
525	259.1	260.6	261.3	266.3	268.5	268.7
580	265.4	265.9	266.5	271.0	273.4	273.5

Table 3 (Continued)

Atmospheric pressure (mbar)	BRINDISI (10:05 G.M.T., April 26, 1970) Spectrum #63, Long 17.8 E, Lat 41.7 N Total water vapor content: 0.9 g cm^{-2}			WALLOPS IS. (15:58 G.M.T., June 25, 1970) Spectrum #37, Long 69.9 W, Lat 38.9 N Total water vapor content: 2.2 g cm^{-2}		
	Radiosonde Temperature Profile (K)	Inversion with water vapor from Radiosonde (K)	Inversion with water vapor abs. correction (K)	Radiosonde Temperature Profile (K)	Inversion with water vapor from Radiosonde (K)	Inversion with water vapor abs. correction (K)
640	271.7	271.0	271.7	275.8	278.3	278.2
707	272.8	276.0	276.6	280.4	283.2	283.0
781	280.1	280.6	281.6	284.5	287.9	287.8
862	285.2	284.7	286.1	288.7	292.2	292.4
952	293.0	288.6	290.5	293.6	292.8	293.7
1013	293.0	286.5	289.4	296.0	293.0	295.2

CONCLUSION

The method developed to account for the water vapor absorption in the inversion of the 15 μm CO_2 band has given satisfactory results. It has been found that the temperature profiles calculated with this method are very close to the temperature profiles obtained using the measured water vapor profile.

The main advantage of the method proposed is that the same two channels in the 11-13 μm window region needed to obtain the corrected surface temperature can be used in a simple scheme to correct the temperature profile for the water vapor absorption effect.

The calculated temperature profiles agree with the radiosonde temperature profiles within the accuracy of the measurements, and show an even better agreement with the profile corrected with the measured water vapor profile.

According with the results obtained, a nine channel radiometer, incorporating seven in the 15 μm CO_2 band and two in the 11-13 μm water vapor window region, can provide a satisfactorily accurate remote temperature sounding.

REFERENCES

Conrath, B. J., Vertical Resolution of Temperature Profiles Obtained from Remote Radiation Measurements, J. Atmos. Sci., Vol. 29, 1262-1271, 1972.

Conrath, B. J., R. A. Hanel, V. G. Kunde and C. Prabhakara, The Infrared Interferometer Experiment on Nimbus 3, J. Geophys. Res. Vol. 75, 5831-5857, 1970.

Hanel, R. A., and B. J. Conrath, Interferometer Experiment on Nimbus 3, Preliminary Results, Science, Vol. 165, 1258-1260, 1969.

Hanel, R. A., B. J. Conrath, V. G. Kunde, C. Prabhakara, I. Revah, V. V. Salomonson, and G. Wolford, The Nimbus 4 Infrared Spectroscopy Experiment, 1. Calibrated Thermal Emission Spectra, J. Geophys. Res., Vol 77, 2629-2641, 1972.

Kunde, V. G., and W. C. Maguire, Direct Integration Transmittance Model, J. Quant. Spectrosc. Radiat. Transfer, Vol 14, 803-817, 1974.

McClatchey, R. A., R. W. Fenn, J. E. A. Selby, F. E. Volz, and J. S. Garing, Optical Properties of the Atmosphere, AFCRL-72-0497, p. 113, Air Force Cambridge Research Laboratories, Bedford, Mass., 1972.

Prabhakara, C., G. Dalu, and V. G. Kunde, Estimation of Sea Surface Temperature From Remote Sensing in the 11-13 μm Window Region, J. Geophys. Res., Vol. 79, 5039-5044, 1974.

Smith, W. L., P. K. Rao, R. Koffler and W. R. Curtis, The Determination of Sea Surface Temperature From Satellite High Resolution Infrared Window Radiation Measurements, Mon. Weather Rev., Vol. 98, No. 8, 604-611, 1970.

Wark, D. Q., SIRS: An Experiment to Measure the Free Air Temperature From a Satellite, Appl. Opt., Vol. 9, 1761-1766, 1970.

Wark, D. Q., and D. T. Hilleary, Atmospheric Temperature: Successful Test of Remote Probing, Science, Vol. 165, 1256-1258, 1969.

FIGURE CAPTIONS

Figure 1. Cloud-free Nimbus 4 IRIS spectrum taken over the ocean on April 27, 1970 at 15.1°N and 144.7°W (GUAM), and the blackbody emission curves. The water vapor transmittance calculated with the radiosonde data is also shown.

Figure 2. Relationship between the function F and the precipitable water content in the atmosphere. T is an example of tropical atmosphere, and MS and MW are midlatitude cases for summer and winter, respectively.

Figure 3. Comparison among the radiosonde temperature profile, the retrieved profile without water vapor correction, and the corrected temperature profile. The IRIS data used are the same presented in Figure 1 (GUAM).